Original article

Nuclear Medicine Communications

# Effects of L-DOPA on striatal iodine-123-FP-CIT binding and behavioral parameters in the rat

Susanne Nikolaus[a], Markus Beu[a], Hubertus Hautzel[a], Angelica M. De Souza Silva[b], Christina Antke[a], Andreas Wirrwar[c], Joseph P. Huston[b] and Hans-Wilhelm Müller[a]

***Purpose*** **The effect of clinical L-3,4-dihydroxyphenylalanine (L-DOPA) doses on the binding of [$^{123}$I]*N*-Ω-fluoropropyl-2β-carbomethoxy-3β-(4-iodophenyl)nortropane ([$^{123}$I]FP-CIT) to the rat dopamine transporter (DAT) was investigated using small animal single-photon emission computed tomography.**

***Materials and methods*** **DAT binding was measured at baseline, after challenge with the aromatic L-amino acid decarboxylase inhibitor benserazide, and after challenge with either 5 or 10 mg/kg L-DOPA plus benserazide. For baseline and challenges, striatal equilibrium ratios ($V_3''$) were computed as an estimation of the binding potential. Moreover, striatal $V_3''$ values were correlated with parameters of motor and exploratory behavior.**

***Results*** **$V_3''$ differed significantly between baseline and either dose of L-DOPA/benserazide. Moreover, $V_3''$ differed significantly between L-DOPA treatment groups. After 5 mg/kg L-DOPA/benserazide, DAT binding was inversely correlated with sitting duration (1–5 min) and sitting frequency (10–15 min). After 10 mg/kg L-DOPA/benserazide, an inverse correlation was found between DAT binding and sitting duration (1–30 min), whereas DAT binding and duration of ambulatory activity (1–30 min) as well as head and shoulder motility (10–15 min) exhibited a positive correlation.**

***Conclusion*** **Challenge with 5 and 10 mg/kg L-DOPA/benserazide led to mean reductions in DAT binding by 34 and 20%, respectively. Results indicate a biphasic response with a higher effect on DAT after the lower dose of L-DOPA. The reduction in DAT binding may be interpreted in terms of competition between [$^{123}$I]FP-CIT and endogenous dopamine. Moreover, there is preliminary evidence of an association between striatal DAT and motor and exploratory parameters.** ***Nucl Med Commun*** **34:1223–1232** © **2013 Wolters Kluwer Health | Lippincott Williams & Wilkins.**

**Nuclear Medicine Communications** 2013, **34:**1223–1232

**Keywords: dopamine transporter, L-3,4-dihydroxyphenylalanine methylester, motor behavior, Parkinson's disease, small animal single-photon emission computed tomography**

[a]Clinic of Nuclear Medicine, University Hospital Düsseldorf, [b]Center for Behavioural Neuroscience, Heinrich-Heine University, Düsseldorf and [c]Department of Nuclear Medicine, Helios Clinic Krefeld GmbH, Krefeld, Germany

Correspondence to Susanne Nikolaus, PhD, Clinic of Nuclear Medicine, University Hospital Düsseldorf, Moorenstr. 5, D-40225 Düsseldorf, Germany
Tel: +49 211 81 17048; fax: +49 211 81 17041;
e-mail: susanne.nikolaus@uni-duesseldorf.de

**Received** 27 June 2013 **Revised** 15 July 2013 **Accepted** 29 July 2013

## Introduction

Presynaptic monoamine transporters such as the dopamine transporter (DAT) regulate signal transduction by controlling neurotransmitter concentrations available for receptor binding at the postsynaptic site. Disturbances in DAT function have been implicated in a variety of disorders including schizophrenia, major depressive disorder, bipolar depression, Tourette's syndrome, attention deficit/hyperactivity disorder, and anxiety disorders (for reviews, see Nikolaus and colleagues [1–3]). Moreover, DAT function is severely impaired in movement disorders including idiopathic and early-onset Parkinson's disease, multiple system atrophy, progressive supranuclear palsy, corticobasal degeneration, Lewy body dementia, and Parkinson's disease dementia (for reviews, see Nikolaus and colleagues [4,5]). As DAT function is altered to different degrees in idiopathic Parkinson's disease and 'Parkinson Plus' syndromes, but not affected in essential tremor [6], DAT imaging with either PET or single-photon emission computed tomography (SPECT) has become an important tool for differentiating between movement disorders.

Symptoms of Parkinson's disease can be ameliorated by treatment with L-3,4-dihydroxyphenylalanine (L-DOPA). Thereby, L-DOPA bypasses the blood–brain barrier through a saturable transporter and is converted to dopamine (DA) by aromatic L-amino acid decarboxylase (AADC) mainly within the presynaptic terminals of striatal DA neurons (for reviews, see Okereke [7]). There is conflicting evidence as to the displaceability of DAT radioligands by endogenous DA: in parkinsonian patients, no significant effect on either [$^{123}$I]*N*-Ω-fluoropropyl-2β-carbomethoxy-3β-(4-iodophenyl) nortropane ([$^{123}$I]FP-CIT) [8] or [$^{123}$I]methyl-3β-(4-iodophenyl)tropane-2β-carboxylate ([$^{123}$I]β-CIT) [9,10] binding was observed after long-term treatment with

0143-3636 © 2013 Wolters Kluwer Health | Lippincott Williams & Wilkins DOI: 10.1097/MNM.0b013e3283657404

L-DOPA in doses of either 150–800 mg/day (plus carbidopa, dose not specified) for 12–72 months [8], 300 mg/day (plus 75 mg/day carbidopa) for up to 46 months [9], or 150, 300, and 600 mg/day (plus 37.5, 75, and 150 mg/day carbidopa) for 10 months [10]. Similar results were obtained by Nurmi *et al.* [11] after long-term treatment with L-DOPA (200–400 mg/day plus carbidopa or benserazide, dose not specified) for 3 months and by Contin *et al.* [12] after acute L-DOPA challenge (100 mg/day plus 25 mg benserazide) with 2β-carbomethoxy-3β-(4-[$^{18}$F]-fluorophenyl)tropane ([$^{18}$F]CFT) and [$^{123}$I]FP-CIT as radioligands. In contrast, Guttman *et al.* [13] observed a significant 16–22% reduction in [$^{11}$C]3β-(4-iodophenyl)tropane-2β-carboxylic acid isopropyl ester ([$^{11}$C]RTI-55) binding after chronic treatment with 300 mg/day L-DOPA (plus 75 mg/day carbidopa) for 6 weeks.

Similarly, ex-vivo dissection studies on rats using [$^{99m}$Tc]TRODAT as the radioligand revealed reductions in DAT binding by 19 and 59% after application of 125 and 150 mg/kg L-DOPA (plus 25 mg/kg benserazide), respectively, and a 44% reduction in DAT binding after application of amphetamine (1.35 mg/kg, [14]). Laruelle *et al.* [15] assessed DAT binding in nonhuman primates after intravenous infusion of L-DOPA (250 μmol/kg plus 5 mg/kg benserazide) or amphetamine (10.8 μmol/kg). In this study, L-DOPA was not found to decrease [$^{123}$I]β-CIT binding, whereas amphetamine reduced [$^{123}$I]β-CIT binding by 50%. More recently, Fernagut *et al.* [16] treated MPTP-lesioned monkeys for 3 months with intravenous infusion of L-DOPA (20 mg/kg twice daily) observing no effect on [$^{99m}$Tc]TRODAT binding compared with controls. In contrast, in a recent small animal PET study on 6-hydroxydopamine (6-OHDA)-lesioned rats, chronic L-DOPA (10 mg/kg plus 15 mg/kg benserazide for 4 weeks) reduced [$^{11}$C]methylphenidate binding by 7% relative to the pretreatment state in the unlesioned contralateral striatum [17]. Interestingly, on the lesioned side, [$^{11}$C]methylphenidate binding was increased by 6% relative to the state before the initiation of treatment.

The finding of reduced DAT binding after pretreatment with L-DOPA or amphetamine may be indicative of a competition between the DAT ligand and synaptic DA. If endogenous DA can displace exogenous radioligands and/or compete with them for presynaptic binding sites, this may have implications for DAT imaging studies on neurologic as well as psychiatric patients receiving DAergic medication. Thus, the rationale of the present study was the assessment of [$^{123}$I]FP-CIT binding to the striatal DAT after challenge with therapeutic doses of L-DOPA (5 or 10 mg/kg). In clinical practice, L-DOPA is administered together with AADC inhibitors such as carbidopa or benserazide to prevent its peripheral conversion to DA (for reviews, see Di Stefano *et al.* [18]). As microdialysis studies have shown that the sole application of benserazide (50 mg/kg) may elevate striatal DA concentrations in normal rats [19], we further assessed [$^{123}$I]FP-CIT binding to the striatal DAT after pretreatment with benserazide. L-DOPA is known to affect motor behavior [20]; therefore, we additionally set out to investigate the association between striatal DAT binding and parameters of motor and exploratory behavior after challenge with 5 or 10 mg/kg of L-DOPA.

## Materials and methods

### Animals

A total of 41 adult male Wistar rats (TVA, Heinrich-Heine University, Düsseldorf, Germany) weighing 398 ± 52 g (mean ± SD) underwent DAT imaging studies at baseline, after treatment with the AADC inhibitor benserazide, and/or after treatment with either 5 or 10 mg/kg L-DOPA plus benserazide. Out of these rats, 19 were subjected to behavioral measurements after administration of 5 or 10 mg/kg L-DOPA with subsequent assessment of DAT binding. On three other rats, images of bone metabolism, soft-tissue perfusion, and brain perfusion were acquired with $^{99m}$Tc-labeled tracers to delineate the striatal and cerebellar target regions as previously published [21,22]. Animals were maintained under standard laboratory conditions with food and water freely available. The study was approved by the regional authority; it was carried out in accordance with the 'Principles of laboratory animal care' (NIH publication No. 86-23, revised 1985) and the German Law on the Protection of Animals.

### Single-photon emission computed tomography camera

The small animal tomograph ('TierSPECT') that was used in the study has been described in detail elsewhere [23]. Tomographic resolutions (full-width at half-maximum) amount to 3.4 and 2.8 mm for $^{123}$I and $^{99m}$Tc, respectively. Sensitivities are 16 cps/MBq ($^{123}$I) and 22 cps/MBq ($^{99m}$Tc). In the present study, a low-energy ultrahigh-resolution parallel-hole collimator ($37 \times 1 \times 0.2\,mm^3$) was mounted in front of the detector head. Data were acquired in a $128 \times 128$ matrix with a pixel width and a slice thickness of $\approx 0.664$ mm. Reconstruction was performed using an iterative ordered-subset expectation maximization algorithm (three iterations, four subsets/iteration). No postfiltering procedure was applied. An attenuation correction of 0.11/cm was implemented for both $^{123}$I and $^{99m}$Tc, assuming a uniformly attenuating medium.

### Dopamine transporter imaging studies

DAT binding was assessed after challenge with 5 mg/kg L-DOPA methylester (Sigma-Aldrich, Taufkirchen, Germany; $n = 15$) plus benserazide (Sigma-Aldrich; dose, 10 mg/kg) or 10 mg/kg L-DOPA methylester plus benserazide ($n = 16$). Of the 15 rats pretreated with 5 mg/kg

L-DOPA/benserazide, all animals underwent DAT imaging at baseline; six animals were scanned further after challenge with benserazide. Of the 16 rats pretreated with 10 mg/kg L-DOPA/benserazide, 14 animals were scanned at baseline, whereas 13 animals additionally underwent DAT imaging after benserazide.

Baseline measurements and measurements after pharmacological challenges were performed in randomized order, and were $11 \pm 7$ days apart. Challenges with benserazide (concentration, 10 mg/ml; vehicle, 0.9% saline) and L-DOPA (concentrations, 5, 10 mg/ml; vehicle, 0.9% saline) plus benserazide (concentration, 10 mg/ml; vehicle, 0.9% saline) were applied intraperitoneally 30 min before radioligand application, as previous investigations in rats had shown that maximum striatal DA concentrations are reached at 30 min after intraperitoneal application of L-DOPA and remain stable for $\sim 2$ h [24]. In the L-DOPA/benserazide condition, L-DOPA and benserazide were administered simultaneously as previous investigations had shown that pretreatment with benserazide up to 3 h before L-DOPA administration did not alter motor responses to L-DOPA compared with concomitant application with the latter compound [25]. Thirty minutes after L-DOPA/benserazide or benserazide application, animals received intraperitoneal injections of 0.9 ml/kg ketamine hydrochloride (Ketavet; Pharmacia GmbH, Erlangen, Germany; concentration, 100 mg/ml) and 0.4 ml/kg xylazine hydrochloride (Rompun; Bayer, Leverkusen, Germany; concentration, *2%*). Into the lateral tail vein, $23 \pm 3$ MBq [$^{123}$I]FP-CIT (Datscan; GE Healthcare, Munich, Germany; concentration range, 0.07–0.13 μg/ml, specific activity range, $2.5–4.5 \times 10^{14}$ Bq/mmol at reference time) was injected using a winged infusion needle set. The tube was rinsed with 1 ml 0.9% saline amounting to a total injection volume of 1.3 ml.

As previous investigations on rats had shown that equilibrium of [$^{123}$I]FP-CIT binding is reached at 2 h post injection with the ratio of specific to nonspecific striatal uptake remaining stable through the following 4 h [26], SPECT measurements were started 2 h after radioligand application. Data acquisition was performed for 60 min. Imaging data were recorded in a step-and-shoot mode over a circular orbit in angular steps of 6° (60 projections, 60 s/projection) using a 65 mm radius of rotation. The 15% energy window was centered on the 159 keV gamma photopeak of $^{123}$I.

Imaging of head and neck bone metabolism, head and neck soft-tissue perfusion, and brain perfusion was performed as previously described [21,22].

### Behavioral studies

Immediately after the injection of either 5 mg/kg ($n = 10$) or 10 mg/kg ($n = 9$) L-DOPA/benserazide, rats were placed into the center of a cage with a top unit equipped with light-emitting diodes and a charge-coupled device camera (Phenotyper; Noldus Information Technology, Wageningen, the Netherlands; open-field dimensions, $45 \times 45 \times 56$ cm). Durations and frequencies of motor (ambulatory activity, sitting without any movement, grooming) and exploratory behaviors (rearing, head and shoulder motility while the animal is sitting or standing) were rated by one of the investigators (S.N.) in blocks of 5 min each for a total of 30 min using EthoVision XT (Noldus Information Technology). Contingent on the behavioral trials, animals were anesthetized and administered [$^{123}$I]FP-CIT as described above.

### Evaluation of dopamine transporter imaging studies

Imaging data were evaluated using the Multi-Purpose-Imaging-Tool (MPI-Tool V3.29; Advanced Tomo Vision GmbH, Kerpen, Germany) as previously described [21,22]. Briefly, target and reference regions were identified using sets of fusion images ([$^{99m}$Tc]DPD-[$^{99m}$Tc]tetrofosmin, [$^{99m}$Tc]DPD-[$^{99m}$Tc]HMPAO, [$^{99m}$Tc]DPD-[$^{123}$I]IFP-CIT), allowing the identification of extracerebral anatomical landmarks such as cranium, orbitae, and Harderian glands and the localization of the respective regions relative to the sites of specific accumulation of metabolic and perfusion markers (Fig. 1a). On coronal slices, striatal target and cerebellar reference regions were defined using the regional activity maxima (Fig. 1b). Thereby, maximum striatal count rates (counts/pixel) were determined on coronal slices by defining a circular region covering an area of 1.5 mm$^2$, which comprised a total of 11 pixels. On the same slices used for the determination of maximum striatal count rates, reference count rates (counts/pixel) were obtained in an elliptic region (area, 7 mm$^2$ comprising a total of 53 pixels) $\sim 15$ mm posterior to the frontal cortex corresponding anatomically to the rat cerebellum. A template of striatal and cerebellar regions was positioned on the individual images by visual inspection without changing their shape or size. Left and right striatal radioactivity concentrations were averaged. For baseline and treatment conditions, the equilibrium ratio of the distribution volumes of the specifically and the nonspecifically bound compartment [$V_3'' = V_T$ (striatum)/$V_T$ (cerebellum) – 1] was computed as an estimate for the binding potential [27].

### Statistical analysis

#### *Dopamine transporter imaging studies*

Distributions of binding data were assessed with the nonparametric Kolmogorov–Smirnov test ($\alpha = 0.05$). Thereby, in each pretreatment condition, $V_3''$ values as well as cerebellar count rates were found to be normally distributed ($0.313 \leq P \leq 0.989$).

Striatal $V_3''$ values and cerebellar radioactivity count rates obtained at baseline, after benserazide, and after 5 or 10 mg/kg L-DOPA/benserazide were compared with

**Fig. 1**

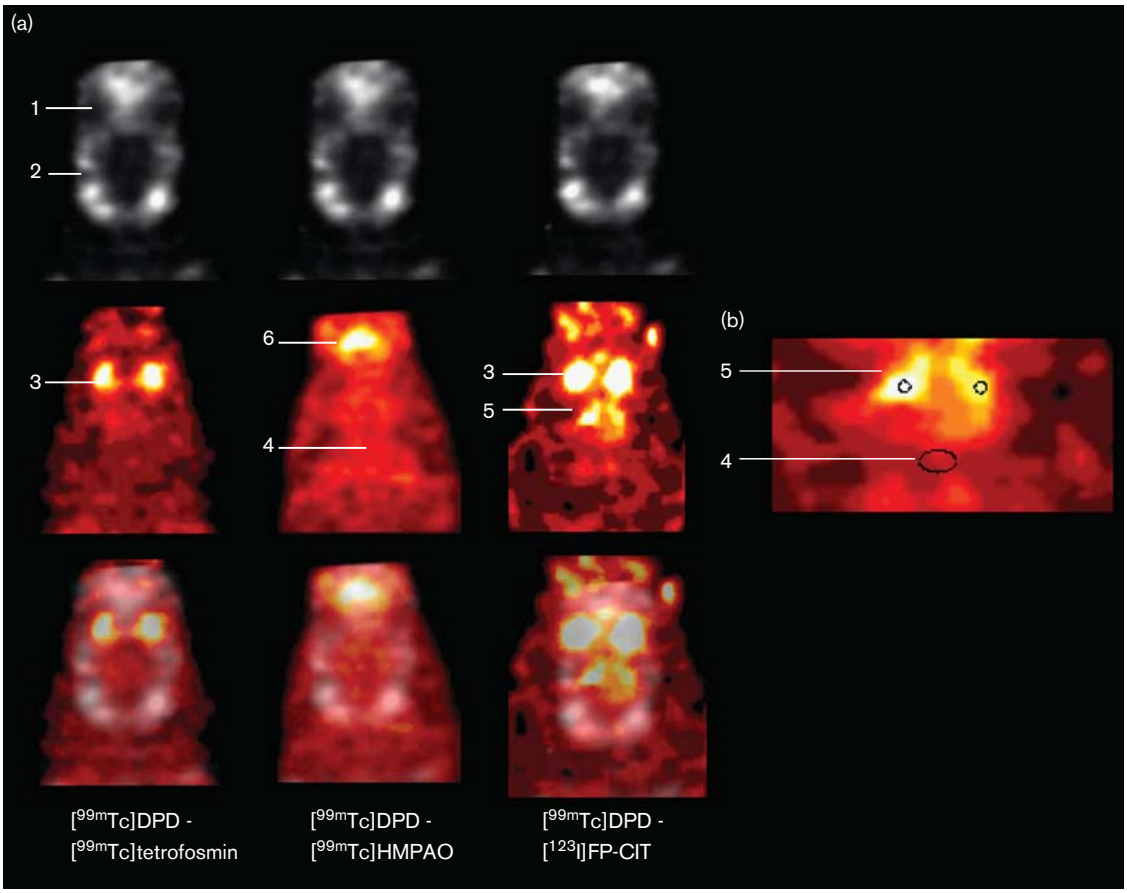


(a) Identification of the rat striatum and cerebellum relative to anatomical landmarks. The left column shows the rat head [$^{99m}$Tc]DPD scan (top), the rat head [$^{99m}$Tc]tetrofosmin scan (middle), and the superimposition of bone metabolism and perfusion scans (below). As these tracers do not pass the blood–brain barrier, their distribution allows the identification of the orbitae (1), cranium (2), and Harderian glands (3). The middle column shows the rat head [$^{99m}$Tc]DPD scan (top), the rat head [$^{99m}$Tc]HMPAO scan (middle), and the superimposition of bone metabolism and brain perfusion scans (below). The fusion of [$^{99m}$Tc]DPD and [$^{99m}$Tc]HMPAO images allows the alignment of the cranium (2) and the cerebral [$^{99m}$Tc]HMPAO accumulation and thus permits the identification of the cerebellum (4) relative to the rat cranium. The right column shows the rat head [$^{99m}$Tc]DPD scan (top), the rat head [$^{123}$I]FP-CIT scan (middle), and the superimposition of [$^{99m}$Tc]DPD and [$^{123}$I]FP-CIT images (below). The fusion image allows the identification of the rat striatum (5) relative to the orbitae (1) and the cranium (2) as visualized by [$^{99m}$Tc]DPD, and to the sites of extracerebral [$^{123}$I]-FP-CIT accumulations corresponding to the sites of extracerebral [$^{99m}$Tc]tetrofosmin accumulations in the Harderian glands (3). Furthermore, the cerebellum (4) may be identified relative to the cranium (2) and to sites of cerebellar (4) HMPAO accumulations. (6) Olfactory mucous membrane. (b) Template consisting of cerebellar (4) and striatal (5) regions of interest. [$^{123}$I]FP-CIT, [$^{123}$I]*N*-Ω-fluoropropyl-2β-carbomethoxy-3β-(4-iodophenyl)nortropane.

one-way analyses of variance (ANOVAs) for repeated measures (Holm–Sidak pairwise multiple comparison, $\alpha = 0.05$). In addition, striatal $V_3''$ values and cerebellar radioactivity count rates were compared between baseline and the respective pretreatment condition (benserazide, 5 mg/kg L-DOPA/benserazide, 10 mg/kg L-DOPA/benserazide) with the paired *t*-test (two tailed, $\alpha = 0.05$). Moreover, striatal $V_3''$ values obtained in L-DOPA/benserazide-treated animals subjected to behavioral analysis were compared between L-DOPA doses using the independent *t*-test (two tailed, $\alpha = 0.05$).

### *Behavioral studies*

Distributions of behavioral data (duration and frequency of ambulatory activity, sitting, rearing, head and shoulder motility, and grooming in minutes 1–5, 6–10, 11–15, 16–20, 21–25, 26–30, and 1–30) were assessed with the nonparametric Kolmogorov–Smirnov test ($\alpha = 0.05$). Thereby, the majority of behavioral parameters were normally distributed in each treatment group ($0.052 \leq P \leq 1$). No normal distribution could be ascertained for rearing duration ($P = 0.032$), rearing frequency ($P = 0.038$), and grooming frequency ($P = 0.047$) during 25–30 min after pretreatment with 5 mg/kg L-DOPA/benserazide and for grooming frequency during 25–30 min after pretreatment with 10 mg/kg L-DOPA/benserazide ($P = 0.045$).

For either treatment group, $V_3''$ values and normally and not normally distributed behavioral data were correlated using the Pearson product moment correlation coefficient

($\alpha = 0.05$) and the Spearman rank correlation (coefficient $\alpha = 0.05$), respectively.

## Results

### Dopamine transporter imaging studies

Figures 2a and 3a show characteristic images of [$^{123}$I]FP-CIT accumulations on coronal slices at baseline and after challenge with 5 mg/kg L-DOPA/benserazide, 10 mg/kg L-DOPA/benserazide, and benserazide alone. Striatal [$^{123}$I]FP-CIT accumulations are markedly reduced following pretreatment with both 5 mg/kg (Fig. 2a) and 10 mg/kg L-DOPA/benserazide (Fig. 3a).

After 5 and 10 mg/kg L-DOPA/benserazide, cerebellar radioactivity concentrations (data not shown) amounted to 812 ± 253 counts/pixel (mean ± SD) and 665 ± 117 counts/pixel, respectively. At baseline, cerebellar radioactivity concentrations of 693 ± 231 counts/pixel (5 mg/kg L-DOPA/benserazide) and 656 ± 173 counts/pixel (10 mg/kg L-DOPA/benserazide) were obtained, whereas after benserazide treatment cerebellar radioactivity concentrations were 797 ± 208 counts/pixel (5 mg/kg L-DOPA/benserazide) and 621 ± 178 counts/pixel (10 mg/kg L-DOPA/benserazide). One-way ANOVAs revealed no significant differences between treatments (5 mg/kg L-DOPA/benserazide, $P = 0.289$; 10 mg/kg L-DOPA/benserazide, $P = 0.901$). Moreover, no significant differences were obtained using paired $t$ tests ($0.089 \leq P \leq 0.922$).

After application of 5 mg/kg (Fig. 2b) and 10 mg/kg L-DOPA/benserazide (Fig. 3b), striatal $V_3''$ was 0.92 ± 0.24 (mean ± SD) and 1.35 ± 0.50, respectively. Baseline $V_3''$ amounted to 1.40 ± 0.42 (5 mg/kg L-DOPA/benserazide) and 1.69 ± 0.44 (10 mg/kg L-DOPA/benserazide), whereas after benserazide $V_3''$ values of 1.17 ± 0.40 (5 mg/kg L-DOPA/benserazide) and 1.62 ± 0.47 (10 mg/kg L-DOPA/benserazide) were obtained. One-way ANOVAs revealed significant differences between treatments (5 mg/kg L-DOPA/benserazide, $P = 0.004$; 10 mg/kg L-DOPA/benserazide, $P = 0.005$). Pairwise multiple comparison procedures yielded $P$ values of 0.001 for both $V_3''$ at baseline versus $V_3''$ after 5 mg/kg L-DOPA/benserazide and for $V_3''$ at baseline versus $V_3''$ after 10 mg/kg L-DOPA/benserazide. Similarly, significant differences were obtained

**Fig. 2**

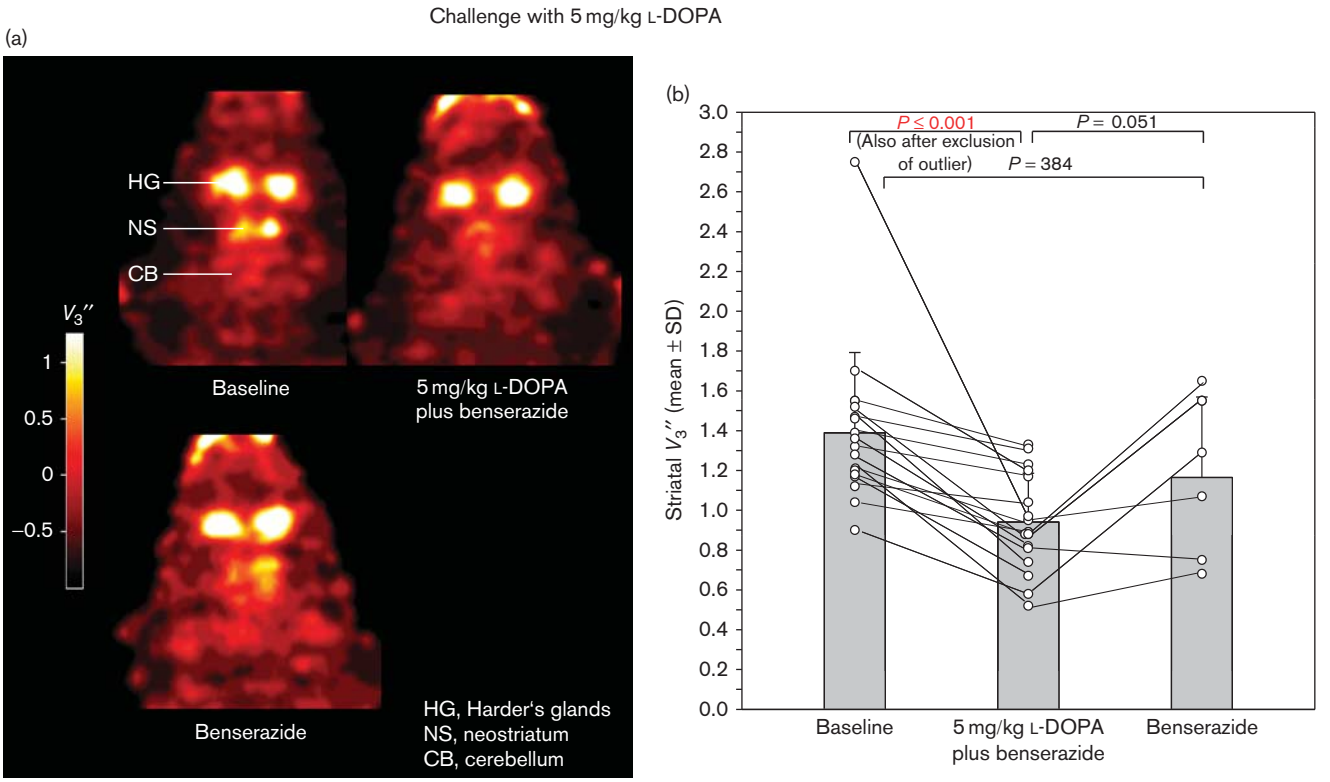


(a) Coronal [$^{123}$I]FP-CIT images of the same rat head at baseline, after pretreatment with 5 mg/kg L-DOPA/benserazide, and after treatment with 10 mg/kg benserazide. The reduction in striatal DAT binding after L-DOPA is clearly visible. All images show $V_3''$ values; it is understood that the calculation of $V_3''$ is only valid for regions of specific radioligand binding such as the rat striatum. Calculations were performed using MATLAB (version 4.2c or version 6; The MathWorks Inc., Novi, Michigan, USA). (b) Striatal equilibrium ratios ($V_3''$) at baseline, after 5 mg/kg L-DOPA/benserazide, and after 10 mg/kg benserazide. Rendered are means and SEM. The circles represent the individual animals. DAT, dopamine transporter; [$^{123}$I]FP-CIT, [$^{123}$I]*N*-Ω-fluoropropyl-2β-carbomethoxy-3β-(4-iodophenyl)nortropane; L-DOPA, L-3,4-dihydroxyphenylalanine.

**Fig. 3**

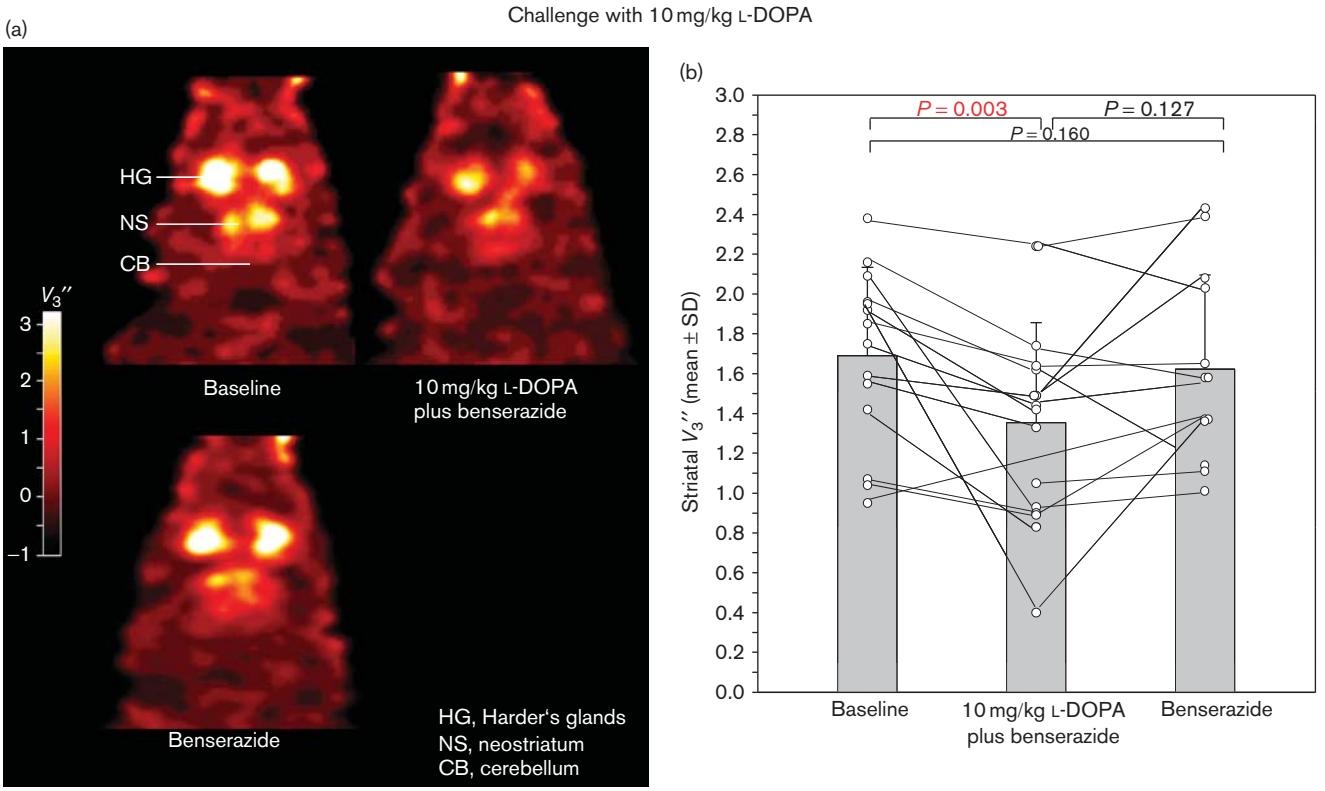


(a) Coronal [$^{123}$I]FP-CIT images of the same rat head at baseline, after pretreatment with 10 mg/kg L-DOPA/benserazide, and after treatment with 10 mg/kg benserazide. The reduction in striatal DAT binding after L-DOPA is clearly visible. All images show $V_3''$ values; it is understood that the calculation of $V_3''$ is valid only for regions of specific radioligand binding such as the rat striatum. Calculations were performed using MATLAB (version 4.2c or version 6; The MathWorks Inc.). (b) Striatal equilibrium ratios ($V_3''$) at baseline, after 10 mg/kg L-DOPA/benserazide, and after 10 mg/kg benserazide. Rendered are means and SEM. The circles represent the individual animals. DAT, dopamine transporter; [$^{123}$I]FP-CIT, [$^{123}$I]*N*-Ω-fluoropropyl-2β-carbomethoxy-3β-(4-iodophenyl)nortropane; L-DOPA, L-3,4-dihydroxyphenylalanine.

between baseline and 5 mg/kg and 10 mg/kg L-DOPA/benserazide ($P = 0.001$ and 0.003, respectively) using paired $t$ tests. If the outlier in the lower dose group (Fig. 2b) is excluded, the difference from baseline remains significant (paired $t$-test; $P < 0.001$). There were no differences between baseline and benserazide conditions or between benserazide and 10 mg/kg L-DOPA/benserazide (paired $t$ tests; $0.127 \leq P \leq 0.384$). For the comparison between benserazide and 5 mg/kg L-DOPA/benserazide, a $P$ of 0.051 was obtained. There were no between-group differences of baseline $V_3''$ (paired $t$ tests; $P = 0.081$). However, $V_3''$ significantly differed between L-DOPA treatment groups (paired $t$ tests; $P = 0.005$).

Also in L-DOPA/benserazide-treated animals subjected to behavioral analysis, striatal $V_3''$ values were significantly different between groups (5 mg/kg L-DOPA/benserazide, $0.90 \pm 0.24$; 10 mg/kg L-DOPA/benserazide, $1.16 \pm 0.30$; $P = 0.047$).

### Behavioral studies

After 5 mg/kg L-DOPA/benserazide, striatal $V_3''$ correlated negatively with rearing duration during 1–5 min ($r = -0.7$, $P = 0.02$) and sitting frequency during 6–15 min ($r = -0.71$, $P = 0.02$). After 10 mg/kg L-DOPA/benserazide, striatal $V_3''$ correlated positively with the durations of ambulatory activity during 1–30 min ($r = 0.67$, $P = 0.05$) and head and shoulder motility during 11–15 min ($r = 0.66$, $P = 0.05$), whereas negative correlations were observed with sitting duration during 1–30 min ($r = -0.068$, $P = 0.045$) and 11–15 min ($r = -0.75$, $P = 0.020$; data not shown).

## Discussion

Challenge with 5 and 10 mg/kg L-DOPA/benserazide led to mean reductions in DAT binding by 34 and 20%, respectively, relative to baseline. The 21% reduction in DAT binding after 5 mg/kg L-DOPA/benserazide relative to benserazide-only treatment was marginally significant. Cerebellar radioactivity concentrations did not differ between baseline and challenges, yielding evidence that under the present experimental conditions no confounding effects were exerted on radioligand accumulation – for example, by affecting cerebral perfusion. As L-DOPA acts by increasing DA efflux (for reviews,

see Misu *et al.* [28]), the reduction in DAT binding may be interpreted in terms of competition between [$^{123}$I]FP-CIT and endogenous DA.

Findings corroborate previous results obtained in humans [13] and rats [14,17]. Moreover, they confirm our findings of reduced DAT binding after application of 25 mg/kg L-DOPA without joint administration of an AADC inhibitor [29]. They are not consistent, however, with the results of Schillaci *et al.* [8], Nurmi *et al.* [11], Contin *et al.* [12], and the Parkinson Study Group [9,10] obtained in humans and with the findings reported by Laruelle *et al.* [15] and Fernagut *et al.* [16] in nonhuman primates.

As mentioned above, only two in-vivo investigations on DAT binding have been conducted in rats contingent on pretreatment with L-DOPA; thereby, Dresel *et al.* [14] determined DAT binding in healthy animals after acute challenge with 125 and 150 mg/kg L-DOPA, whereas Sossi *et al.* [17] assessed DAT binding in 6-OHDA-lesioned rats after long-term treatment with 10 mg/kg L-DOPA. Findings obtained in both studies are qualitatively consistent with the results of the present investigation. However, in the study by Sossi *et al.* [17], chronic application of the same dose (10 mg/kg L-DOPA) led to a 7% reduction in DAT binding, whereas in the present investigation a much higher decrease of 20% was observed. This may be accounted for by the differences in methodologies: whereas in our study DAT binding was measured after acute treatment with L-DOPA, Sossi *et al.* [17] administered L-DOPA chronically over 4 weeks, which may have induced compensatory mechanisms including a reduction in DA release over the course of time. Moreover, in the study by Dresel *et al.* [14], application of the much higher doses of 125 and 150 mg/kg L-DOPA reduced DAT binding by 19 and 59%, whereas in our study pretreatment with 5 and 10 mg/kg decreased DAT binding by 34 and 20%, respectively, relative to baseline. These observations imply that doses of L-DOPA in the therapeutic range may be sufficient to markedly increase synaptic DA.

After treatment with L-DOPA, Sossi *et al.* [17] observed a decrease in DAT binding in the intact contralateral striatum of rats with unilateral nigrostriatal 6-OHDA lesions, but an increase in DAT binding was observed on the lesioned side. It may be conjectured that the lesion-induced decrease in striatal DA concentration elevated ipsilateral DAT binding relative to the contralateral side because of reduced competition with radioligand molecules. This conclusion is supported by our own result of decreased DAT binding in healthy animals, and also by the fact that in studies on lesioned nonhuman primates DAT binding was not reduced upon pretreatment with L-DOPA [15,16]. It appears that the number of DAT binding sites after L-DOPA depends on the extent of nigrostriatal degeneration in two respects: the process of neurodegeneration, first, leads to a progressive reduction of DAT binding sites and, second, diminishes the capacity to synthesize and release DA contingent on administration of the precursor molecule. As a consequence, the reduction in radioligand binding after treatment with L-DOPA may be related to the severity of symptoms. This is underlined by the fact that parkinsonian patients who displayed a significant decrease in DAT binding after long-term treatment with L-DOPA had a Unified Parkinson's Disease Rating Scale score of 23.9 ± 6.0 [13], whereas in those investigations in which no alterations in DAT binding were observed Unified Parkinson's Disease Rating Scale scores were higher, amounting to 35.1 ± 11.8 [8], 31.0 ± 48.0 [11], 25.3 ± 12.0 [12], 30.6 ± 11.4 [9], and 28.0 ± 13.0 [10]. This implies that disease severity must be taken into account in in-vivo investigations assessing the effect of DAergic treatments on constituents of the DAergic synapse. This not only pertains to Parkinson's disease but also to other disorders affecting the DAergic system, including schizophrenia, depression, and anxiety disorders (for reviews, see Nikolaus and colleagues [1–3]).

In the present study, absolute $V_3''$ values differed significantly between animals administered 5 and 10 mg/kg L-DOPA/benserazide. This was also the case in L-DOPA/benserazide-treated animals subjected to behavioral analysis. These results indicate a biphasic response with a higher effect on DAT after the lower dose of L-DOPA. Biphasic regulatory actions of L-DOPA on DA and other neurotransmitters including noradrenaline and acetylcholine are widely known (for review, see Misu *et al.* [30]); *in vitro*, nanomolar concentrations of L-DOPA were repeatedly found to facilitate DA release, whereas micromolar concentrations exerted inhibitory effects [28,31–33]. *In vivo*, a comparison across studies provides less consistent results, with reports of either similar efficacy of 6 mg/kg [34] and 12 mg/kg L-DOPA [35], or increased efficacy of either 6 mg/kg [36] or 25 mg/kg L-DOPA [37] relative to the 12 mg/kg dose [35]. These findings, however, are not comparable to our results, as the challenging doses between 6 and 25 mg/kg were applied to 6-OHDA-lesioned rats, and contingent on chronic administration of 5–25 mg/kg L-DOPA injected once or twice daily over 10–14 days [34–37]. Therefore, further studies over a wider dose range and, in particular, after long-term treatment with L-DOPA will help to elucidate the regulatory mechanisms underlying DA synthesis and release with respect to applied dose and duration of treatment. The latter may be of special interest given the high incidence of dyskinesias, motor fluctuations, and 'wearing off' phenomena in parkinsonian patients under chronic L-DOPA therapy (for review, see Cenci *et al.* [38]).

The observed biphasic action of L-DOPA raises the question as to by which mechanisms the disparate effects

on DA efflux and DAT binding are exerted. Apparently, in the present study, 5 mg/kg L-DOPA increased synaptic DA levels relative to the 10 mg/kg dose, leading to increased competition between endogenous DA and the exogenous radioligand for DAT binding sites. DA release is modulated by a negative feedback loop, which is established by DA acting upon presynaptic terminal autoreceptors of the inhibitory $D_{2/3}$ receptor subtype (for reviews, see Langer [39]). Thus, it is conceivable that DA concentrations after 10 mg/kg L-DOPA at the time of radioligand application were lower compared with the 5 mg/kg dose, because, in the 30 min time span between injection of L-DOPA and application of [$^{123}$I]FP-CIT, the higher dose may have promoted the release of DA in concentrations sufficient to activate feedback inhibition at the presynaptic terminal. This agrees with the in-vitro findings of Misu *et al.* [28], who observed a blockade of DA release after micromolar relative to nanomolar concentrations of L-DOPA mediated by $D_2$ autoreceptor binding. Matters, however, may be even more complicated: Misu *et al.* [28], for instance, attributed the abolition of DA efflux to direct action of L-DOPA on presynaptic $D_2$ receptor binding sites rather than to feedback inhibition exerted by newly released DA molecules. In addition, after nanomolar concentrations of L-DOPA, DA release was facilitated by interaction with excitatory presynaptic β-adrenoreceptors [28]. Further, previous studies have shown that L-DOPA may inhibit acetylcholine efflux [40] and facilitate the release of both glutamate [41] and γ-amino acid butyric acid ([42]). Interaction of L-DOPA with other neurotransmitter systems also includes L-DOPA decarboxylation in striatal serotonin (5-HT) neurons [43] with subsequent DA storage in presynaptic vesicles [44] and its release into the synaptic cleft [45]. As DA neurons are modulated by all of these neurotransmitters (ACh [46], glutamate [47], γ-amino acid butyric acid [48], and 5-HT [49]), further investigations are needed to clarify which synaptic site of which neurotransmitter system is challenged by which dose of L-DOPA and whether DA levels or the concentrations of its precursor are relevant for the induction of either forward inhibition or activation of the presynaptic feedback loop.

To our knowledge, we present the first in-vivo evidence on the association between DAT binding and parameters of motor and exploratory behavior. Thereby, in the group administered 5 mg/kg, lower DAT binding predicted longer rearing behavior during 1–5 min and higher sitting frequency during 11–15 min. In the group administered 10 mg/kg, lower DAT binding predicted decreased head and shoulder motility during 11–15 min and less ambulation and more sitting throughout the trial. These results indicate an association between striatal DAT and motor and exploratory parameters, which appear to be both behavior-specific and time-dependent. In addition, our results may reflect an inter-relation with endogenous DA: as L-DOPA increased DA concentrations (and decreased DAT binding), it may be that higher DA levels (reflected by lower DAT binding) decreased behavioral activity, whereas lower DA levels (reflected by higher DAT binding) had the opposite effects. Further investigations with a higher number of animals are required to thoroughly assess behavioral parameters together with DAT binding over a wider range of L-DOPA doses. Moreover, as motor behavior in adult rats has been related to striatal $D_2$ receptor function [50] our studies in the near future will be complemented with the joint assessment of behavioral parameters and $D_2$ receptor after challenge with L-DOPA.

Two limitations of our study must be taken into account: first, previous investigations have shown that radioactivity concentrations *in vivo* may be underestimated because of partial-volume effects [51]. Possible are also overestimations of radioactivity concentrations caused by spillover from the Harderian glands. The latter may be the case in more rostral striatal regions, whereas the former hampers radioactivity quantification in thin structures like caudal striatal portions. As neither a partial-volume nor a spillover correction was performed in our study, quantification of striatal radioactivity counts may have been confounded relative to cerebellar radioactivity counts, as this structure due to its largeness and caudal localization is subject to neither effect. Moreover, as no exact anatomical coregistration was possible, it cannot be ruled out that positioning of regions of interest and reference regions did not slightly vary between animals or even between treatment conditions in the same animal. Second, [$^{99m}$Tc]DPD, [$^{99m}$Tc]tetrofosmin, and [$^{99m}$Tc]HMPAO scans were performed on rats other than those scanned with [$^{123}$I]FP-CIT. To minimize intersubject variation, however, animals of the same strain and age were used. Further, rats were positioned in a custom-built head holder (Institute of Medicine, Research Center Jülich, Jülich, Germany) to ensure reproducible positioning of the animals within the field of view. Notably, notwithstanding these limitations, quantitative data obtained with our small animal tomograph are conclusive in that they confirm both qualitatively and quantitatively the findings of L-DOPA-induced reduction of DAT binding in both humans [13] and rats [14].

It may be argued that, in view of the limited spatial resolution of small animal SPECT, ex-vivo autoradiography or immunohistochemistry might represent more suitable methods for the assessment of DAT after pharmacological challenges. However, the use of ex-vivo methods precludes the performance of more than one trial on a single animal, whereas in-vivo approaches such as small animal SPECT permit the use of each rat as its own control. As a consequence, data do not have to be pooled from several animals and tested for significance between groups; instead, the possible influence of

intersubject variation may be reduced by the performance of pre–post comparisons. Besides, due to inherent methodological problems such as variations in slice thickness or cellular destruction in the cryosections ('quenching') also ex-vivo methods are not supposed to yield error-free results, apart from the fact that it is debatable, in as much as findings obtained *ex vivo* on frozen brain slices may reflect the conditions, functions, and mechanisms in the brain of a living animal.

In the present investigation, L-DOPA was administered together with the AADC inhibitor benserazide. Previous findings obtained with in-vivo microdialysis have shown that a single administration of L-DOPA (50 mg/kg) with vehicle pretreatment instead of application of benserazide increase extracellular DA by 560% [24]. Furthermore, although the combination of L-DOPA and benserazide led to a higher increase in extracellular DA levels compared with L-DOPA (50 mg/kg) alone, the sole application of benserazide (50 mg/kg) also induced a pronounced elevation in striatal DA [19]. Therefore, it is likely that even the relatively low dose of benserazide (10 mg/kg) applied in the present study contributed to our findings obtained after 5 and 10 mg/kg L-DOPA by increasing extracellular DA concentrations. This is supported by the fact that in the present investigation benserazide led to a – although nonsignificant – reduction in DAT binding relative to baseline. Moreover, DAT binding after both 5 and 10 mg/kg L-DOPA/benserazide was decreased relative to benserazide-only treatment, with the difference between 5 mg/kg L-DOPA/benserazide and the benserazide-only condition exhibiting a marginal significance. Besides, in a previous investigation, pretreatment with 25 mg/kg L-DOPA without joint application of benserazide reduced [$^{123}$I]FP-CIT binding to the striatal DAT by 20% [29]. Additional investigations on DAT binding after varying doses of benserazide should be conducted to shed further light on this matter. In addition, studies on 6-OHDA-lesioned rats should be conducted to gauge the effects of L-DOPA with and without benserazide in relation to unlesioned animals. This is important as parkinsonian patients under chronic L-DOPA therapy receive concomitant treatment with some AADC inhibitor, and effects on the outcome of DAT-SPECT may be due to the concurring actions of both types of compounds.

## Conclusion

Taken together, findings yield evidence that therapeutic doses of L-DOPA can notably reduce [$^{123}$I]FP-CIT binding to the DAT. Results indicate a biphasic response with a higher effect on DAT after the lower dose of L-DOPA. The reduction in DAT binding may be interpreted in terms of competition between [$^{123}$I]FP-CIT and endogenous DA. Moreover, there is evidence of an association between striatal DAT and motor and exploratory parameters, which appears to be both behavior-specific and time-dependent. Further in-vivo investigations on normal rats and on parkinsonian lesion models after chronic L-DOPA may be helpful in clarifying whether, and under which circumstances, the present findings have implications for the performance of DAT-SPECT in neurologic and psychiatric patients receiving DAergic medications.

## Acknowledgements

A. M. De Souza Silva and J. P. Huston were supported by the 'Deutsche Forschungsgemeinschaft' (Grant number: DFG DE 792/2–4) and by a Grant from ERA-Net NEURON 'Development and advancement in methods and technologies towards the understanding of brain diseases'. Furthermore, we gratefully acknowledge the technical support received from R. Engels from the Central Laboratory of Electronics (Research Center Jülich, Jülich, Germany).

### Conflicts of interest

There are no conflicts of interest.

## References

1 Nikolaus S, Antke C, Müller HW. In vivo imaging of synaptic function in the central nervous system. II. Mental and affective disorders. *Behav Brain Res* 2009; **204**:32–66.
2 Nikolaus S, Beu M, Antke C, Müller HW. Cortical GABA, striatal dopamine and midbrain serotonin as the key players in compulsive and anxiety disorders – results from in vivo imaging studies. *Rev Neurosci* 2010; **21**:119–139.
3 Nikolaus S, Hautzel H, Heinzel A, Müller HW. Key players in major and bipolar depression – a retrospective analysis of in vivo imaging studies. *Behav Brain Res* 2012; **232**:358–390.
4 Nikolaus S, Antke C, Kley K, Poeppel TD, Hautzel H, Schmidt D, Müller HW. Investigating the dopaminergic synapse in vivo. I. Molecular imaging studies in humans. *Rev Neurosci* 2007; **18**:439–472.
5 Nikolaus S, Antke C, Müller HW. In vivo imaging of synaptic function in the central nervous system. I. Movement disorders and dementia. *Behav Brain Res* 2009; **204**:1–31.
6 Plotkin M, Amthauer H, Klaffke S, Kühn A, Lüdemann L, Arnold G, *et al.* Combined $^{123}$I-FP-CIT and $^{123}$I-IBZM SPECT for the diagnosis of Parkinsonian syndromes: study on 72 patients. *J Neural Transm* 2005; **112**:677–692.
7 Okereke CS. Role of integrative pharmacokinetic and pharmacodynamic optimization strategy in the management of Parkinson's disease patients experiencing motor fluctuations with levodopa. *J Pharm Pharm Sci* 2002; **5**:146–161.
8 Schillaci O, Pierantozzi M, Filippi L, Manni C, Brusa L, Danieli R, *et al.* The effect of levodopa therapy on dopamine transporter SPECT imaging with (123)I-FP-CIT in patients with Parkinson's disease. *Eur J Nucl Med Mol Imaging* 2005; **32**:1452–1456.
9 Parkinson Study Group. Dopamine transporter brain imaging to assess the effects of pramipexole vs. levodopa on Parkinson's disease progression. *JAMA* 2002; **287**:1653–1661.
10 Parkinson Study Group. Levodopa and the progression of Parkinson's disease. *N Engl J Med* 2004; **46**:2498–2508.
11 Nurmi E, Bergman J, Eskola O, Solin O, Hinkka SM, Sonninen P, Rinne JO. Reproducibility and effect of levodopa on dopamine transporter function measurements: a [$^{18}$F]CFT PET study. *J Cereb Blood Flow Metab* 2000; **20**:1604–1609.
12 Contin M, Martinelli P, Mochi M, Albani F, Riva R, Scaglione C, *et al.* Dopamine transporter gene polymorphism, SPECT imaging, and levodopa response in patients with Parkinson disease. *Clin Neuropharmacol* 2004; **27**:111–115.
13 Guttman M, Stewart D, Hussey D, Wilson A, Houle S, Kish S. Influence of L-dopa and pramipexole on striatal dopamine transporter in early PD. *Neurology* 2001; **56**:1559–1564.

14 Dresel SH, Kung MP, Plossl K, Meegalla SK, Kung HF. Pharmacological effects of dopaminergic drugs on in vivo binding of [$^{99m}$Tc]TRODAT-1 to the central dopamine transporters in rats. *Eur J Nucl Med* 1998; **25**:31–93.
15 Laruelle M, Baldwin M, Malison RT, Zea-Ponce Y, Zoghbi SS, al-Tikriti MS, *et al*. SPECT imaging of dopamine and serotonin transporters with [$^{123}$I]beta-CIT: pharmacological characterization of brain uptake in nonhuman primates. *Synapse* 1993; **13**:295–309.
16 Fernagut PO, Li Q, Dovero S, Chan P, Wu T, Ravenscroft P, *et al*. Dopamine transporter binding is unaffected by L-DOPA administration in normal and MPTP-treated monkeys. *PLoS One* 2010; **5**:e14053.
17 Sossi V, Dinelle K, Schulzer M, Mak E, Doudet DJ, de la Fuente-Fernandez R. Levodopa and pramipexole effects on presynaptic dopamine PET markers and estimated dopamine release. *Eur J Nucl Med Mol Imaging* 2010; **37**:2364–2370.
18 Di Stefano A, Sozio P, Cerasa LS, Iannitelli A. L-Dopa prodrugs: an overview of trends for improving Parkinson's disease treatment. *Curr Pharm Des* 2011; **17**:3482–3493.
19 Silva MA, Mattern C, Häcker R, Tomaz C, Huston JP, RKW Schwarting. Increased neostriatal dopamine activity after intraperitoneal or intranasal administration of L-DOPA: on the role of benserazide pretreatment. *Synapse* 1997; **27**:294–302.
20 Chao OY, Mattern C, Silva AM, Wessler J, Ruocco LA, Nikolaus S, *et al*. Intranasally applied L-DOPA alleviates Parkinsonian symptoms in rats with unilateral nigro-striatal 6-OHDA lesions. *Brain Res Bull* 2012; **87**:340–345.
21 Nikolaus S, Wirrwar A, Kley K, Antke C, Müller HW. In vivo quantification of dose-dependent dopamine transporter blockade in the rat striatum with small animal SPECT. *Nucl Med Commun* 2007; **28**:207–213.
22 Nikolaus S, Beu M, Antke C, Kley K, Wirrwar A, Huston JP, Müller HW. Binding of [$^{123}$I]iodobenzamide to the rat D2 receptor after challenge with methylphenidate assessed with a dedicated small animal SPECT. *Eur J Nucl Med Mol Imaging* 2011; **38**:694–701.
23 Schramm N, Wirrwar A, Sonnenberg F, Halling H. Compact high resolution detector for small animal SPECT. *IEEE Trans Nucl Sci* 2000; **47**: 1163–1166.
24 Shen H, Kannari K, Yamato H, Arai A, Matsunaga M. Effects of benserazide on L-DOPA-derived extracellular dopamine levels and aromatic L-amino acid decarboxylase activity in the striatum of 6-hydroxydopamine-lesioned rats. *Tohoku J Exp Med* 2003; **199**:149–159.
25 Tayarani-Binazir KA, Jackson MJ, Fisher R, Zoubiane G, Rose S, Jenner P. The timing of administration, dose dependence and efficacy of dopa decarboxylase inhibitors on the reversal of motor disability produced by L-DOPA in the MPTP-treated common marmoset. *Eur J Pharmacol* 2010; **635**:109–116.
26 Booi J, Andringa G, Rijks LJ, Vermeulen RJ, De Bruin K, Boer GJ, *et al*. [$^{123}$I]FP-CIT binds to the dopamine transporter as assessed by biodistribution studies in rats and SPECT studies in MPTP-lesioned monkeys. *Synapse* 1997; **27**:183–190.
27 Laruelle M, van Dyck C, Abi-Dargham A, Zea-Ponce Y, Zoghbi SS, Charney DS, *et al*. Compartmental modeling of iodine-123-iodobenzofuran binding to dopamine D2 receptors in healthy subjects. *J Nucl Med* 1994; **35**:743–754.
28 Misu Y, Goshima Y, Kubo T. Biphasic actions of L-DOPA on the release of endogenous dopamine via presynaptic receptors in rat striatal slices. *Neurosci Lett* 1986; **72**:194–198.
29 Nikolaus S, Larisch R, Vosberg H, Beu M, Wirrwar A, Kley K, *et al*. Pharmacological challenge and synaptic response – assessing dopaminergic function in the rat striatum with small animal SPECT and PET. *Rev Neurosci* 2011; **22**:625–645.
30 Misu Y, Goshima Y, Ueda H, Okamura H. Neurobiology of L-DOPAergic systems. *Prog Neurobiol* 1996; **49**:415–454.
31 Goshima Y, Nakamura S, Misu Y. L-Dopa facilitates the release of endogenous norepinephrine and dopamine via presynaptic beta 1- and beta 2-adrenoceptors under essentially complete inhibition of L-aromatic amino acid decarboxylase in rat hypothalamic slices. *Jpn J Pharmacol* 1990; **53**:47–56.
32 Goshima Y, Misu Y, Arai N, Misugi K. Nanomolar L-dopa facilitates release of dopamine via presynaptic beta-adrenoceptors: comparative studies on the actions in striatal slices from control and 1-methyl-4-phenyl-1,2,3,6-tetrahydropyridine (MPTP)-treated C57 black mice, an animal model for Parkinson's disease. *Jpn J Pharmacol* 1991; **55**:93–100.
33 Arai N, Misugi K, Goshima Y, Misu Y. Evaluation of a 1-methyl-4-phenyl-1,2,3,6-tetrahydropyridine (MPTP)-treated C57 black mouse model for Parkinsonism. *Brain Res* 1990; **515**:57–63.
34 Lundblad M, af Bjerkén S, Cenci MA, Pomerleau F, Gerhardt GA, Strömberg I. Chronic intermittent L-DOPA treatment induces changes in dopamine release. *J Neurochem* 2009; **108**:998–1008.
35 Navailles S, Bioulac B, Gross C, De Deurwaerdère P. Chronic L-DOPA therapy alters central serotonergic function and L-DOPA-induced dopamine release in a region-dependent manner in a rat model of Parkinson's disease. *Neurobiol Dis* 2011; **41**:585–590.
36 Lindgren HS, Andersson DR, Lagerkvist S, Nissbrandt H, Cenci MA. L-DOPA-induced dopamine efflux in the striatum and the substantia nigra in a rat model of Parkinson's disease: temporal and quantitative relationship to the expression of dyskinesia. *J Neurochem* 2010; **112**:1465–1476.
37 Meissner W, Ravenscroft P, Reese R, Harnack D, Morgenstern R, Kupsch A, *et al*. Increased slow oscillatory activity in substantia nigra pars reticulata triggers abnormal involuntary movements in the 6-OHDA-lesioned rat in the presence of excessive extracellular striatal dopamine. *Neurobiol Dis* 2006; **22**:586–598.
38 Cenci MA, Ohlin KE, Odin P. Current options and future possibilities for the treatment of dyskinesia and motor fluctuations in Parkinson's disease. *CNS Neurol Disord Drug Targets* 2011; **10**:670–684.
39 Langer SZ. 25 years since the discovery of presynaptic receptors: present knowledge and future perspectives. *Trends Pharmacol Sci* 1997; **18**: 95–99.
40 Ueda H, Sato K, Okumura F, Misu Y. L-DOPA inhibits spontaneous acetylcholine release from the striatum of experimental Parkinson's model rats. *Brain Res* 1995; **698**:213–216.
41 Goshima Y, Ohno K, Nakamura S, Miyamae T, Misu Y, Akaike A. L-DOPA induces Ca-dependent and tetrodotoxin-sensitive release of of endogenous glutamate from rat striatal slices. *Brain Res* 1993; **617**:167–170.
42 Misu Y, Yue JL, Okumura Y, Miyamae T, Goshima Y. Interactions between endogenous L-DOPA and GABAA systems for cardiovascular control in the rat nucleus tractus solitarii. In: Tanaka C, Bowery NG, editors. *GABA: receptor, transporters and metabolism*. Basel: Birkhäuser Verlag; 1995. pp. 115–121.
43 Ng KY, Chase TN, Colburn RW, Kopin IJ. L-Dopa-induced release of cerebral monoamines. *Science* 1970; **170**:76–77.
44 Miller DW, Abercrombie ED. Role of high-affinity dopamine uptake and impulse activity in the appearance of extracellular dopamine in striatum after administration of exogenous L-DOPA: studies in intact and 6-hydroxydopamine-treated rats. *J Neurochem* 1999; **72**:1516–1522.
45 Tanaka H, Kannari K, Maeda T, Tomiyama M, Suda T, Matsunaga M. Role of serotonergic neurons in L-DOPA-derived extracellular dopamine in the striatum of 6-OHDA-lesioned rats. *Neuroreport* 1999; **10**:631–634.
46 Giorguieff MF, Le Floch ML. Presynaptic receptors of nicotinic and muscarinic types in the control of the spontaneous release of DA from striatal dopaminergic terminals in the rat. *J Pharmacol Exp Ther* 1990; **200**:535–544.
47 Scott L, Kruse MS, Forssberg H, Brismar H, Greengard P, Aperia A. Selective up-regulation of dopamine D1 receptors in dendritic spines by NMDA receptor activation. *Proc Natl Acad Sci USA* 2002; **99**:1661–1664.
48 Grace AA, Bunney BS. Paradoxical GABA excitation of nigral dopaminergic cells: indirect mediation through reticulata inhibitory neurons. *Eur J Pharmacol* 1979; **59**:211–218.
49 Alex KD, Pehek EA. Pharmacologic mechanisms of serotonergic regulation of dopamine neurotransmission. *Pharmacol Ther* 2007; **113**:296–320.
50 Helmeste DM. Spontaneous and apomorphine-induced locomotor changes parallel dopamine receptor differences in two rat strains. *Pharmacol Biochem Behav* 1983; **19**:153–155.
51 Nikolaus S, Beu M, Vosberg H, Müller HW, Larisch R. Quantitative analysis of dopamine D2 receptor kinetics with small animal positron emission tomography. *Methods Enzymol* 2004; **385**:228–239.